HTS 2020 Modelling

7th International Workshop on Numerical Modelling of High-Temperature Superconductors

22nd-23rd June 2021
Virtual (Nancy, France)

2D Numerical Simulations of HTS Stacks of Tapes for Cable-in-Conduit Conductor Cables

G. De Marzi*, G. Celentano, A. Augieri, M. Marchetti, and A. Vannozzi

ENEA - Department of Fusion and Technology for Nuclear Safety and Security
Frascati Research Center, Via Enrico Fermi 45, 00044 Frascati, Rome (Italy)

ENEA
Italian National Agency for New Technologies, Energy and Sustainable Economic Development

EUROfusion

BACKGROUND

Cable-in-conduit conductors comprised of twisted stacks of HTS tapes [1, 2] with aluminium slotted core constitute a very promising technology by virtue of their easy manufacturing process, flexibility capabilities, and high current densities. Currently, applications in the nuclear fusion industry of this HTS cable concept are being considered for the improvement of DTT and DEMO reactor performances.

The current distribution among tapes is one of the key parameters affecting the cable performances [3]. We here present a 2D finite-element model [4], which computes the magnetic field and current distribution in stacked tapes. This model can be also used to describe the experimental *V-I* results obtained in cables in which different current distributions among tapes are expected.

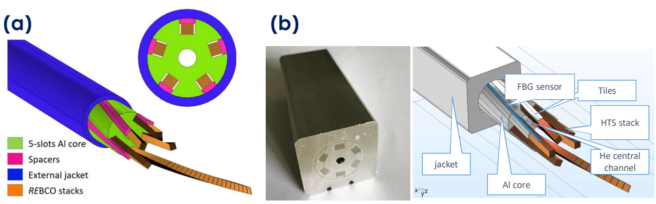

Figure 1. HTS CICCs currently being developed at ENEA: (a) 5-slot round cable; (b) 6-slot round-in-square.

METHODOLOGY

- The **T-A formulation** of the Maxwell's equations [5] is a well-established model, and it has already been applied to a variety of HTS devices, such as coils [6] and cables [7, 8]
- The state variables are the current vector potential T, and the magnetic vector potential A; ***A*** is defined all over the bounded universe, while ***T*** is exclusively defined along the superconducting medium
- *Thin strip approximation*: the superconducting tapes are modeled as 1D objects
- Transport currents are applied by a proper choice of the boundary conditions for ***T***:

$$\nabla \times \rho \nabla \times \boldsymbol{T} = -\partial_t \boldsymbol{B}$$

$$\nabla \times \nabla \times \boldsymbol{A} = \mu \boldsymbol{J}$$

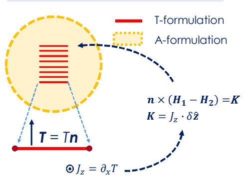

$$I = \iint_{\Sigma} \nabla \times \boldsymbol{T} \cdot d\boldsymbol{S} = \int_{\Lambda} \boldsymbol{T} \cdot d\boldsymbol{l}$$

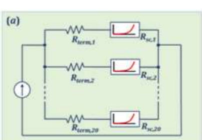

$$\rho_{sc,k} = \frac{E_c}{J_{c,k}} \left(\frac{J_k}{J_{c,k}} \right)^{n_k - 1}$$

$$\rho = \left(\frac{1}{\rho_{sc}} + \frac{1}{\rho_n} \right)^{-1} + \rho_{term}$$

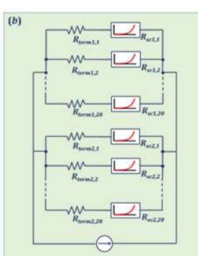

This approximation is valid when tape-to-tape contact resistance is higher than the tape termination resistance as likely occurs for sample of lab-scale length

SIMULATIONS AND COMPARISON WITH EXPERIMENTS

Experiment #1: stack of 20 tapes

Cu-stabilized tape Pro-Line TPL4300c, by THEVA, has been used (Table I). The investigated 1-m-long CICC sample is comprised by one stack of 20 HTS tapes and four dummy stacks of Stainless Steel (SS) tapes.

Table I Experiments #1 and #2: main parameters of the HTS tape and CICC cable (*w* = width; *t* = thickness).

Parameter	Sample
HTS tape[a]	THEVA TPL4300c
Tape size (*w* x *t*) [mm x mm]	3.4 x 0.15
Substrate, thickness [mm]	Hastelloy C-276, 0.1
Cu stabilizer's thickness [μm]	20 (per side)
I_c [A], 77 K self-field	~160
Twist pitch [mm]	∞
Core diameter [mm]	19
Number of slots	5
Slot size (*w* x *h*) [mm x mm]	4.3 x 4.3
Number of HTS stacks	1 (*Exp. #1*), 2(*Exp. #2*)
Number of tapes per HTS stack	20
Number of dummy stacks	4 (*Exp. #1*), 3(*Exp. #2*)
Dummy tape, (*w* x *t*) [mm x mm]	SS, 4.0 x 0.15

[a] From Datasheets provided by supplier.

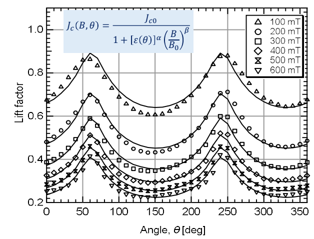

Figure 2. Lift factor [8] of tape TPL2300c as a function of *θ* for different fields, T = 77 K (markers). Lines represent the fits to the Equation reported in the inset.

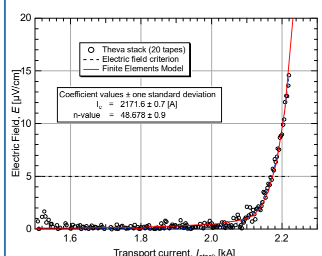

Figure 3. *E–I* characteristic: *markers*= measured; *line*: FE simulation. Values for I_c and *n*-index are calculated by fit to the power-law $E = E_c(I/I_c)^n$.

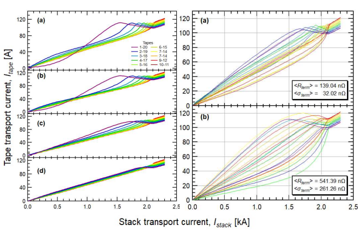

Figure 4. Individual tape current as a function of cable current. Left side: R_{term} is equal for all tapes in the stack: (a) 1 nΩ; (b) 10 nΩ; (c) 100 nΩ; (d) 500 nΩ. Right side: gaussian distributed random values of R_{term}, with standard deviations of: (a) 32 nΩ; (b) 261 nΩ.

For $I \ll I_c$, the current repartition is governed by the R_{term} values and the inductance distribution among tapes, whereas self-field effects become dominant for $I \lessapprox I_c$. In spite of R_{term} variations by more than two orders of magnitude, the shape of the *E-I* characteristic curve of figure 3 does not change.

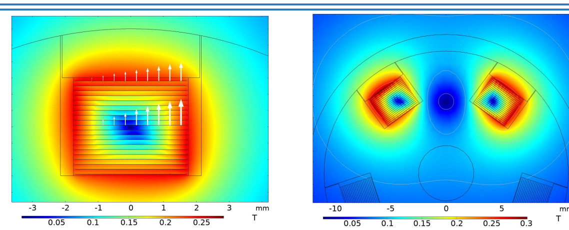

Figure 5. Magnetic field maps calculated with the *T-A formulation* close to the superconducting-to-normal transition region. Left: field map for the single THEVA stack (Experiment #1). The direction and relative magnitude of the current vector potential ***T*** is plotted for two selected tapes, one on the top and the other in the middle of the stack (white arrows); right: field map for two adjacent THEVA stacks (Experiment #2).

Experiment #2: two adjacent stacks of 20 tapes

To study the current distribution among different stacks within the CICC, we made a second cable very similar to the one used in Experiment #1, using the same THEVA tapes.

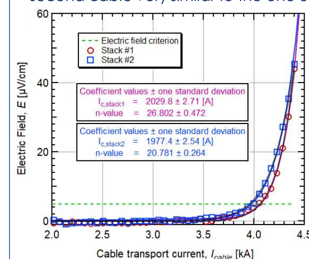

The critical currents of the stacks differ by about 50 A. This can be explained in terms of different superconducting properties of the two stacks (i.e., different <I_c> and <n-index>) and by a reduced current sharing between the two stacks.

Figure 6. Measured *E–I* curves of the cable with two superconducting stacks (open markers). Continuous and dotted lines represent the Finite Element solution and the fit to the power law, respectively.

Experiment #3: bent stack

To study the effect of the variation of I_c among tapes, we have analyzed the current distribution in a 1-meter cable which has been bent down to R_b = 0.15 m (see Table II).

Table II Experiment #3: main parameters of the HTS tape and CICC cable (*w* = width; *t* = thickness).

Parameter	Sample
HTS tape[a]	SuNAM SCN04150
Tape size (*w* x *t*) [mm x mm]	4.0 x 0.15
Substrate, thickness [mm]	Stainless steel, 0.1
Cu stabilizer's thickness [μm]	20 (per side)
Average I_c [A], 77 K self-field[a]	245
Twist pitch [mm]	500
Core diameter [mm]	19
Number of slots	5
Slot size (*w* x *h*) [mm x mm]	4.3 x 4.3
Number of tapes per HTS stack	20
Dummy tape, (*w* x *t*) [mm x mm]	SS, 4.0 x 0.15
Wrapping tape, (*w* x *t*) [mm x mm]	40 x 0.1
External jacket, thickness [mm]	Al tube, 1.25

[a] From Datasheets provided by supplier.

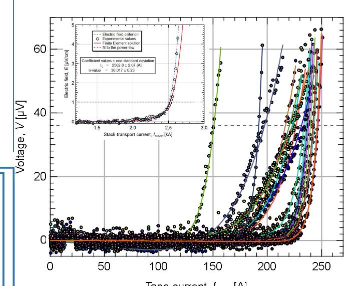

Figure 7. Full set of *V–I* curves measured individually on each tape of the bent SuNAM stack. Inset: Characteristic curve of the whole stack.

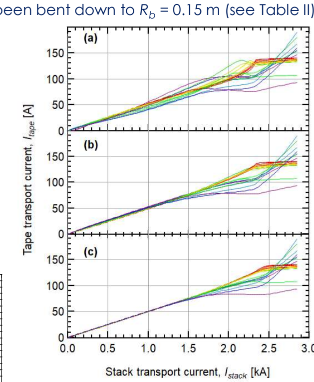

Figure 8. Individual tape current as a function of cable current for three different value of R_{term}: (a) 10 nΩ; (b) 100 nΩ; (c) 500 nΩ.

Some of the tapes entered the current sharing regime well before the transition to the normal phase of the whole stack, and the current distribution was highly uneven. In spite of this, the stack showed good electrical stability.

REFERENCES

[1] G. De Marzi *et al.*, IEEE TAS **26** (4), 4801607 (2016)
[2] G. Celentano *et al.*, IEEE TAS **24** (3), 4601805 (2013)
[3] V. Pothavajhala *et al.*, IEEE TAS **24** (3), 4800505 (2013)
[4] G. De Marzi *et al.*, SuST **34**, 035016 (2021)
[5] H. Zhang *et al.*, SuST **30**, 024005 (2017)
[6] F. Liang *et al.*, J. Appl. Phys. **122** (4), 043903 (2017)
[6] S. Fu *et al.*, IEEE TAS **28** (4), 4802005 (2018)
[7] Y. Wang *et al.*, SuST **32** (2), 025003 (2019)
[8] Y. Liu et al., SuST 32, 014001 (2019)